# Pathway Analysis of Gene Expression in Murine Fetal and Adult Wounds

Michael S. Hu, Wan Xing Hong, Michael Januszyk, Graham G. Walmsley, Anna Luan, Zeshaan N. Maan, Shawn Moshrefi, Ruth Tevlin, Derrick C. Wan, Geoffrey C. Gurtner, Michael T. Longaker, and H. Peter Lorenz*

*Division of Plastic Surgery, Hagey Laboratory for Pediatric Regenerative Medicine, Department of Surgery, Stanford University School of Medicine, Stanford, California.*

*This abstract has been presented at the 8th Annual Academic Surgical Congress on February 5–7, 2013 in New Orleans, Louisiana and the 26th Annual Meeting of the Wound Healing Society on April 23–27, 2014 in Orlando, Florida.*

H. Peter Lorenz, MD

Submitted for publication January 29, 2018. Accepted in revised form January 29, 2018.

*Correspondence: Division of Plastic Surgery, Hagey Laboratory for Pediatric Regenerative Medicine, Department of Surgery, Stanford University School of Medicine, 257 Campus Drive, Stanford, CA 94305-5148
(e-mail: plorenz@stanford.edu).

**Objective:** In early gestation, fetal wounds heal without fibrosis in a process resembling regeneration. Elucidating this remarkable mechanism can result in tremendous benefits to prevent scarring. Fetal mouse cutaneous wounds before embryonic day (E)18 heal without scar. Herein, we analyze expression profiles of fetal and postnatal wounds utilizing updated gene annotations and pathway analysis to further delineate between repair and regeneration.
**Approach:** Dorsal wounds from time-dated pregnant BALB/c mouse fetuses and adult mice at various time points were collected. Total RNA was isolated and microarray analysis was performed using chips with 42,000 genes. Significance analysis of microarrays was utilized to select genes with >2-fold expression differences with a false discovery rate of <2. Enrichment analysis was performed on significant genes to identify differentially expressed pathways.
**Results:** Our analysis identified 471 differentially expressed genes in fetal versus adult wounds following injury. Utilizing enrichment analysis of significant genes, we identified the top 20 signaling pathways that were upregulated and downregulated at 1 and 12 h after injury. At 24 h after injury, we discovered 18 signaling pathways upregulated in adult wounds and 11 pathways upregulated in fetal wounds.
**Innovation:** These novel target genes and pathways may reveal repair mechanisms of the early fetus that promote regeneration over fibrosis.
**Conclusion:** Our microarray analysis recognizes hundreds of possible genes as candidates for regulators of scarless versus scarring wound repair. Enrichment analysis reveals 109 signaling pathways related to fetal scarless wound healing.

**Keywords:** wound healing, scarless repair, regeneration, microarray

## INTRODUCTION

A LANDMARK REPORT by Rowlatt in 1979 described that human fetuses in early gestation heal wounds without scar formation in a process resembling regeneration.[1] Since then, this remarkable regenerative ability has been demonstrated across a number of mammalian species.[2–4] Although key differences have been identified between fetal scarless wound regeneration and adult scarring wound repair, the exact mechanism remains largely unknown.[5] We previously characterized the gene expression profile of fetal and adult wounds at



DOI: 10.1089/wound.2017.0779

numerous time points following injury.[6] However, owing to an outdated gene database and limited methods of analysis, the results of the study were difficult to extrapolate for further research. Herein, we perform gene expression analysis with updated gene annotations on embryonic day (E)17 scarless fetal and scarring adult mouse wounds. Moreover, we perform enrichment pathway analysis to identify functional molecular pathways differentially expressed between scarless and scarring repair. With identification of these pathways, many of which are novel to wound regeneration, we aim to provide new targets for promoting scarless wound healing.

## CLINICAL PROBLEM ADDRESSED

Adult cutaneous wounds heal through a fibroproliferative response that results in incomplete regeneration of the original tissue.[7] There is an overproduction of an unorganized collagen meshwork with loss of dermal appendages.[8] The resultant scar tissue is weaker and has a tensile strength <80% of the original form.[9] This highly evolved process, although efficient in protecting from infection, further injury, and water loss, can be problematic. In the pediatric population, scars can restrict growth and impede movement when they occur across joints. Furthermore, scars occurring in locations such as the face can lead to devastating psychological and social consequences. In addition, humans can develop pathological scars, such as keloids or hypertrophic scars, when wound healing occurs rampantly. This results in a scar that is characterized by excessive disorganized collagen deposition and is raised, cosmetically unpleasing, and often associated with symptoms such as pain and itching.[10] The ability to prevent such scar formation and promote wounds to undergo regeneration would be highly beneficial to healthcare and society, by easing the tremendous clinical burden of scarring and fibrosis estimated to be in the tens of billions of dollars.[9]

## MATERIALS AND METHODS

### Animals

Six-week-old wild-type BALB/c mice were purchased from Charles River Laboratories (Wilmington, MA) and housed at 22°C with a 12-h day/12-h night cycle. All animals received water and normal chow *ad libitum*. For timed gestations, the mice were bred overnight and the day of vaginal plug was considered E0.5 day of gestation. Animals were maintained in the Stanford Animal Care Laboratory and all procedures were conducted in accordance with university-approved protocols according to National Institutes of Health (NIH) guidelines.

### Fetal mouse wounding

Fetal wounding was performed as previously described.[11] Briefly, pregnant mice (gestational age E17) were utilized. After induction of anesthesia, midline laparotomy was performed using microsurgical scissors. The uterus and fetus selected for surgery were gently exposed using cotton-tip applicators. The surgical field was irrigated with warm (38°C) phosphate-buffered saline (PBS). The fetus was carefully positioned to allow access to the dorsum. A purse-string stitch using a 7-0 nylon suture was passed through the uterus overlying the site of intended dorsal wounding. A 3 mm incision was made through the uterine wall and amniotic sac in the center of the purse-string stitch. Using microsurgical scissors, a single full-thickness excisional wound, $\sim$1 mm in diameter, was created on the dorsum of the fetus. The wound was marked with India ink. Warm (38°C) PBS was injected into the amniotic sac with a blunt-tipped 10-guage syringe as the purse string was closed and the syringe was carefully retracted. One fetus of unknown gender per litter was wounded. The peritoneal cavity was irrigated with warm (38°C) PBS. The peritoneum and abdominal skin were everted, reapproximated, and stapled closed. Prior studies from our laboratory have shown that the histology of these wounds reveal complete regeneration within 48 h. Hematoxylin and eosin and trichrome staining reveal rapid reepithelialization and normal collagen architecture.[12] Thus, time points less than 48 h were chosen for analysis of wounds. The pregnant mice were sacrificed and fetal wounds were harvested at 1, 12, and 24 h ($n=3$ for each time point) following wounding by excising the wound with a 2 mm rim of surrounding tissue using microsurgical scissors, as previously described.[6] An equivalent amount of tissue from the contralateral dorsum of the same fetus was collected in the same manner for normalization.

### Adult mouse wounding

For adult wounding, 2 mm excisional wounds were generated on the back of 3-week-old BALB/c mice of mixed gender using punch biopsy after induction of anesthesia and preparation for aseptic surgery, as described above for pregnant mice. Mice were sacrificed and wounds were harvested at 1, 12, and 24 h ($n=3$ for each time point) following injury for comparison to fetal wounds. Wounds were harvested by excising the wound along with a 2 mm rim of normal tissue by punch biopsy for

reproducibility, as previously described.[6] An equivalent amount of tissue from the contralateral dorsum of the same fetus was collected in the same manner for normalization. The larger size wound, which is a fourfold increase in area, accounts for an approximately fourfold size discrepancy between the fetal and postnatal wound. However, despite the differences in wound size, the relative wound to body size in the fetal and postnatal mouse is not the same and may confound our data.

### RNA extraction and amplification

RNA from fetal and adult wounds at various time points was extracted using the Trizol protocol (Invitrogen, Carlsbad, CA) as per manufacturer's instructions and as previously described.[13] One microgram of RNA from each experimental sample ($n = 3$ per group per time point) was amplified. One-microgram aliquots of universal mouse RNA were amplified in individual reaction mixtures and utilized as internal amplification controls.

### Preparation of fluorescent complementary DNA probes

Fluorescent complementary DNA (cDNA) probes were prepared as previously described.[13]

### Pretreatment of microarray chips

The Stanford Microarray Database Center was used to print mouse microarray chips with 42,000 specific cDNAs printed onto each lysine-coated slide. These cDNAs represent single accession numbers from Genbank (sequences and accession numbers of the cDNAs can be found on http://genome-www5.stanford.edu//index.shtml). Before hybridization, microarray chips were rehydrated, snap-dried, and crosslinked as previously described.[13]

### Microarray hybridization

Microarray hybridization was performed as previously described.[13]

### Microarray data analysis

Scanned images were analyzed using the Genepix Pro 4.0 software (Molecular Devices), as previously described.[13] Significance analysis of microarrays (SAM) was used to select genes with significant expression differences between the E17 fetal and adult wound transcriptomes for each time point. Genes that had at least a twofold expression difference with false discovery rate <2 were selected.

### Functional analysis of differentially expressed genes

To identify functional connections among significantly regulated genes, both network and pathway analyses of the probes filtered by microarray were performed using Ingenuity Pathways Analysis (Ingenuity Systems, Redwood City, CA), as previously described.[13]

## RESULTS

### Differential gene expression between adult and fetal wounds

Wound microarray data were normalized to age-matched unwounded control skin (taken from the contralateral dorsum of the same fetus/adult during wound collection) data sets. Normalized transcriptomes from E17 fetal wounds were directly compared to normalized transcriptomes from adult wounds. SAM identified 471 differentially expressed genes with greater than twofold difference between E17 fetal and adult wounds at 1, 12, and 24 h postinjury. At 1 h following wounding, 178 genes were upregulated in E17 fetal wounds, whereas 13 genes were downregulated when compared to adult wounds (Table 1). At 12 h following injury, E17 fetal wounds upregulated 112 genes, whereas adult wounds upregulated 141 genes (Table 2). Twenty-four hours postwounding, 16 genes were downregulated in E17 fetal wounds and 11 genes were upregulated versus adult wounds (Table 3).

### Functional pathway analysis

Analysis of the 178 genes found to be upregulated in E17 fetal wounds at 1 h postinjury resulted in the identification of 20 functional pathways (Fig. 1B). The top five pathways were associated with the following: proline biosynthesis, arginine degradation, mevalonate pathway, and Parkinson's signaling. Utilizing the 13 downregulated genes in E17 fetal wounds, a list of 20 functional pathways were again identified (Fig. 1C). The top five pathways were as follows: interleukin (IL)-8 signaling, mechanistic target of rapamycin signaling, glucocorticoid receptor signaling, regulation of IL-2 expression in activated and anergic T lymphocytes, and T cell receptor signaling.

At 12 h following injury, out of 112 genes upregulated in E17 fetal wounds, 20 pathways were identified (Fig. 2B). The top five pathways were related to apoptosis, role of osteoblasts, osteoclasts and chondrocytes in rheumatoid arthritis, Ras-related nuclear protein signaling, and protein ubiquitination pathway. Conversely, of 141 genes upregulated in adult wounds at 12 h, 20 functional pathways (Fig. 2C) reveal the top five to include the thioredoxin pathway, CXC chemokine receptor (CXCR)4 signaling, IL-1 signaling, Cdc42 signaling, and vitamin C transport.

Gene expression of E17 fetal and adult wounds at 24 h after injury reveal 27 differentially expressed

**Table 1.** *Differentially expressed genes in embryonic day 17 fetal versus adult wounds at one hour postwounding*

| *Gene Symbol* | *Gene Name* | *Regulation* |
|---|---|---|
| Cd177 | CD177 antigen | Up |
| Runx1t1 | Translocated to, 1 (cyclin D related) | Up |
| Ndufa3 | NADH dehydrogenase (ubiquinone) 1 alpha subcomplex, 3 | Up |
| Mettl21a | Methyltransferase like 21A | Up |
| Sfn | Stratifin | Up |
| Agfg1 | ArfGAP with FG repeats 1 | Up |
| Tpd52l1 | Tumor protein D52-like 1 | Up |
| Abcb1b | ATP-binding cassette, subfamily B (MDR/TAP), member 1B | Up |
| Cab39 | Calcium binding protein 39 | Up |
| AU019823 | Expressed sequence AU019823 | Up |
| Chst11 | Carbohydrate sulfotransferase 11 | Up |
| Tspo | Translocator protein | Up |
| Pex3 | Peroxisomal biogenesis factor 3 | Up |
| Rps6ka3 | Ribosomal protein S6 kinase polypeptide 3 | Up |
| Myc | Myelocytomatosis oncogene | Up |
| Aco1 | Aconitase 1 | Up |
| Mtf1 | Metal response element binding transcription factor 1 | Up |
| Fchsd2 | FCH and double SH3 domains 2 | Up |
| Ccdc106 | Coiled-coil domain containing 106 | Up |
| Ptgs1 | Prostaglandin endoperoxide synthase 1 | Up |
| Vegfa | Vascular endothelial growth factor A | Up |
| Tbc1d22a | TBC1 domain family, member 22a | Up |
| Cd34 | CD34 antigen | Up |
| Nos2 | Nitric oxide synthase 2, inducible | Up |
| Riok1 | RIO kinase 1 (yeast) | Up |
| Agl | Amylo-1,6-glucosidase, 4-alpha-glucanotransferase | Up |
| Fam38a | Family with sequence similarity 38, member A | Up |
| Tmem184b | Transmembrane protein 184b | Up |
| Ensa | Endosulfine alpha | Up |
| Mll1 | Myeloid/lymphoid or mixed-lineage leukemia 1 | Up |
| Rps13 | Ribosomal protein S13 | Up |
| Cmc1 | COX assembly mitochondrial protein homolog (*Saccharomyces cerevisiae*) | Up |
| Hdlbp | High-density lipoprotein (HDL) binding protein | Up |
| Rps13 | Ribosomal protein S13 | Up |
| Btg3 | B cell translocation gene 3 | Up |
| Gal | Galanin | Up |
| Gigyf2 | GRB10 interacting GYF protein 2 | Up |
| Csda | Cold shock domain protein A | Up |
| Anpep | Alanyl (membrane) aminopeptidase | Up |
| Icmt | Isoprenylcysteine carboxyl methyltransferase | Up |
| Abr | Active BCR-related gene | Up |
| Pank3 | Pantothenate kinase 3 | Up |
| Pbx1 | Pre-B cell leukemia transcription factor 1 | Up |
| Snx10 | Sorting nexin 10 | Up |
| Mycbp | c-myc binding protein | Up |
| CACNA1S | Calcium channel, voltage-dependent, L type, alpha 1S subunit | Up |
| Rps15a | Ribosomal protein S15A | Up |
| Dffb | DNA fragmentation factor, beta subunit | Up |
| Rorc | RAR-related orphan receptor gamma | Up |
| Grb2 | Growth factor receptor bound protein 2 | Up |
| Wiz | Widely-interspaced zinc finger motifs | Up |
| Hic2 | Hypermethylated in cancer 2 | Up |
| Ngly1 | *N*-glycanase 1 | Up |
| Cast | Calpastatin | Up |
| Ptgs2 | Prostaglandin-endoperoxide synthase 2 | Up |
| Zfp106 | Zinc finger protein 106 | Up |
| Atxn1l | Ataxin 1 like | Up |
| Ing5 | Inhibitor of growth family, member 5 | Up |
| Sorbs1 | Sorbin and SH3 domain-containing 1 | Up |
| Fndc3b | Fibronectin type III domain containing 3B | Up |
| Sult1d1 | Sulfotransferase family 1D, member 1 | Up |
| Rac1 | RAS-related C3 botulinum substrate 1 | Up |
| Scarb2 | Scavenger receptor class B, member 2 | Up |
| Ak3 | Adenylate kinase 3 | Up |
| Mrpl16 | Mitochondrial ribosomal protein L16 | Up |
| Maneal | Mannosidase, endo-alpha like | Up |
| Slc25a18 | Solute carrier family 25 (mitochondrial carrier), member 18 | Up |
| Chrac1 | Chromatin accessibility complex 1 | Up |
| Fbln1 | Fibulin 1 | Up |
| Pnck | Pregnancy upregulated nonubiquitously expressed CaM kinase | Up |
| Cdkn2aip | CDKN2A interacting protein | Up |
| Kcna1 | Potassium voltage-gated channel, shaker-related subfamily, member 1 | Up |
| Crnkl1 | Crn, crooked neck-like 1 (*Drosophila*) | Up |
| Ikbkb | Inhibitor of kappaB kinase beta | Up |
| Trim44 | Tripartite motif-containing 44 | Up |
| Etfa | Electron transferring flavoprotein, alpha polypeptide | Up |
| Vdac1 | Voltage-dependent anion channel 1 | Up |
| Porcn | Porcupine homolog (*Drosophila*) | Up |
| Glo1 | Glyoxalase 1 | Up |
| Pln | Phospholamban | Up |
| Ablim2 | Actin-binding LIM protein 2 | Up |
| Clip1 | CAP-GLY domain containing linker protein 1 | Up |
| LTC4S | Leukotriene C4 synthase | Up |
| Cybb | Cytochrome *b*-245, beta polypeptide | Up |
| Cmbl | Carboxymethylenebutenolidase like (*Pseudomonas*) | Up |
| Col11a2 | Collagen, type XI, alpha 2 | Up |
| Il10rb | Interleukin 10 receptor, beta | Up |
| Pacsin1 | Protein kinase C and casein kinase substrate in neurons 1 | Up |
| Rasl11a | RAS-like, family 11, member A | Up |
| Calm1 | Calmodulin 1 | Up |
| Sirt5 | Sirtuin 5 (silent mating type information regulation 2 homolog) 5 (*S. cerevisiae*) | Up |
| Rhbdd3 | Rhomboid domain containing 3 | Up |
| Ggt1 | Gamma-glutamyltransferase 1 | Up |
| Mmgt2 | Membrane magnesium transporter 2 | Up |
| Ccdc90b | Coiled-coil domain containing 90B | Up |
| Igf2 | Insulin-like growth factor 2 | Up |
| Fbxo5 | F-box protein 5 | Up |
| Ppp2r3d | Protein phosphatase 2 (formerly 2A), regulatory subunit B″, delta | Up |
| Kcne2 | Potassium voltage-gated channel, Isk-related subfamily, gene 2 | Up |
| Ndrg4 | N-myc downstream regulated gene 4 | Up |
| Vcp | Valosin=containing protein | Up |
| Stat5b | Signal transducer and activator of transcription 5B | Up |
| Try4 | Trypsin 4 | Up |
| Pdia6 | Protein disulfide isomerase associated 6 | Up |
| Spcs2 | Signal peptidase complex subunit 2 homolog (*S. cerevisiae*) | Up |
| Spag7 | Sperm-associated antigen 7 | Up |
| Me1 | Malic enzyme 1, NADP(+)-dependent, cytosolic | Up |
| BC018507 | cDNA sequence BC018507 | Up |

(*continued*)

**Table 1.** (*Continued*)

(*continued*)

**Table 1. (*Continued*)**

| Gene Symbol | Gene Name | Regulation |
|---|---|---|
| Cbx5 | Chromobox homolog 5 (*Drosophila* HP1a) | Up |
| Ano5 | Anoctamin 5 | Up |
| Zfp61 | Zinc finger protein 61 | Up |
| Crlf1 | Cytokine receptor-like factor 1 | Up |
| Dkc1 | Dyskeratosis congenita 1, dyskerin homolog (human) | Up |
| Aff4 | AF4/FMR2 family, member 4 | Up |
| Ptprb | Protein tyrosine phosphatase, receptor type, B | Up |
| Eif4 h | Eukaryotic translation initiation factor 4H | Up |
| Mapkapk5 | MAP kinase-activated protein kinase 5 | Up |
| Rpl18a | Ribosomal protein L18A | Up |
| Keg1 | Kidney expressed gene 1 | Up |
| Pcf11 | Cleavage and polyadenylation factor subunit homolog (*S. cerevisiae*) | Up |
| Prr5 | Proline rich 5 (renal) | Up |
| Rcn3 | Reticulocalbin 3, EF-hand calcium binding domain | Up |
| Bola1 | Bola-like 1 (*Escherichia coli*) | Up |
| B3gat3 | Beta-1,3-glucuronyltransferase 3 (glucuronosyltransferase I) | Up |
| Got2 | Glutamate oxaloacetate transaminase 2, mitochondrial | Up |
| Copz1 | Coatomer protein complex, subunit zeta 1 | Up |
| Cox17 | Cytochrome *c* oxidase, subunit XVII assembly protein homolog (yeast) | Up |
| Sf3b3 | Splicing factor 3b, subunit 3 | Up |
| Lims2 | LIM and senescent cell antigen-like domains 2 | Up |
| Fam3a | Family with sequence similarity 3, member A | Up |
| Bphl | Biphenyl hydrolase-like (serine hydrolase, breast epithelial mucin-associated antigen) | Up |
| Odam | Odontogenic, ameloblast associated | Up |
| Ly6 g6e | Lymphocyte antigen 6 complex, locus G6E | Up |
| Rps15 | Ribosomal protein S15 | Up |
| Far2 | Fatty acyl CoA reductase 2 | Up |
| Ndufc2 | NADH dehydrogenase (ubiquinone) 1, subcomplex unknown, 2 | Up |
| Crip1 | Cysteine-rich protein 1 (intestinal) | Up |
| Rer1 | RER1 retention in endoplasmic reticulum 1 homolog (*S. cerevisiae*) | Up |
| Stra13 | Stimulated by retinoic acid 13 | Up |
| Mpv17l2 | MPV17 mitochondrial membrane protein-like 2 | Up |
| Nfatc3 | Nuclear factor of activated T cells, cytoplasmic, calcineurin-dependent 3 | Up |
| Mcam | Melanoma cell adhesion molecule | Up |
| Gnb2l1 | Guanine nucleotide binding protein (G protein), beta polypeptide 2 like 1 | Up |
| Slc12a2 | Solute carrier family 12, member 2 | Up |
| Rps3 | Ribosomal protein S3 | Up |
| Cda | Cytidine deaminase | Up |
| Ccnd3 | Cyclin D3 | Up |
| Wipf1 | WAS/WASL interacting protein family, member 1 | Up |
| Dhps | Deoxyhypusine synthase | Up |
| Cbr1 | Carbonyl reductase 1 | Up |
| Rapgef4 | Rap guanine nucleotide exchange factor (GEF) 4 | Up |
| Itgb2 | Integrin beta 2 | Up |
| Sgk1 | Serum/glucocorticoid regulated kinase 1 | Up |
| Phf17 | PHD finger protein 17 | Up |
| Mxd3 | Max dimerization protein 3 | Up |
| Car10 | Carbonic anhydrase 10 | Up |
| Commd10 | COMM domain containing 10 | Up |
| Uck2 | Uridine–cytidine kinase 2 | Up |
| Ccl6 | Chemokine (C–C motif) ligand 6 | Up |
| Neu1 | Neuraminidase 1 | Up |
| Zfp735 | Zinc finger protein 735 | Up |
| Anxa10 | Annexin A10 | Up |
| Meis2 | Meis homeobox 2 | Up |
| Mtx1 | Metaxin 1 | Up |
| Mtfp1 | Mitochondrial fission process 1 | Up |
| Kpna3 | Karyopherin (importin) alpha 3 | Up |
| Pole3 | Polymerase (DNA directed), epsilon 3 (p17 subunit) | Up |
| Gstk1 | Glutathione S-transferase kappa 1 | Up |
| Trpm1 | Transient receptor potential cation channel, subfamily M, member 1 | Up |
| Baz2b | Bromodomain adjacent to zinc finger domain, 2B | Up |
| Igf1 | Insulin-like growth factor 1 | Up |
| Vps37a | Vacuolar protein sorting 37A (yeast) | Up |
| Atp5 g1 | ATP synthase, H+ transporting, mitochondrial F0 complex, subunit c1 (subunit 9) | Up |
| Prdm2 | PR domain containing 2, with ZNF domain | Up |
| Ube2z | Ubiquitin-conjugating enzyme E2Z (putative) | Up |
| Srp72 | Signal recognition particle 72 | Up |
| Pim2 | Proviral integration site 2 | Up |
| Ccng1 | Cyclin G1 | Up |
| Ncaph2 | Non-SMC condensin II complex, subunit H2 | Down |
| Actc1 | Actin, alpha, cardiac muscle 1 | Down |
| Acaa2 | Acetyl-Coenzyme A acyltransferase 2 (mitochondrial 3-oxoacyl-Coenzyme A thiolase) | Down |
| Pycrl | Pyrroline-5-carboxylate reductase like | Down |
| Tcfcp2l1 | Transcription factor CP2-like 1 | Down |
| Hmgcr | Transcribed locus | Down |
| Gab1 | Growth factor receptor bound protein 2-associated protein 1 | Down |
| Mtmr9 | Myotubularin-related protein 9 | Down |
| Uchl1 | Ubiquitin carboxy-terminal hydrolase L1 | Down |
| Tsn | Translin | Down |
| Uba3 | Ubiquitin-like modifier activating enzyme 3 | Down |
| Nsun4 | NOL1/NOP2/Sun domain family, member 4 | Down |
| Zbtb8a | Zinc finger and BTB domain containing 8a | Down |

genes. Of the 16 downregulated in E17 fetal wounds, 18 pathways were distinguished (Fig. 3B). Eumelanin biosynthesis, transfer RNA (tRNA) charging, glial cell line-derived neurotrophic factor family ligand–receptor interactions, neurotrophin/tropomyosin receptor kinase (TRK) signaling, and platelet-derived growth factor signaling comprise the top five pathways. From the 11 genes upregulated in the fetal wounds, 11 pathways were identified to be relevant to fetal wound healing (Fig. 3C). The top five functional pathways include dolichol and dolichyl phosphate biosynthesis, intrinsic prothrombin activation pathway, chronic myeloid leukemia signaling, IL-6 signaling, and atherosclerosis signaling.

## DISCUSSION

Fetal cutaneous wound healing is uniquely characterized by scarless repair with full restoration

**Table 2.** *Differentially expressed genes in embryonic day 17 fetal versus adult wounds at twelve hours postwounding*

| *Gene Symbol* | *Gene Name* | *Regulation* |
|---|---|---|
| Nck1 | Noncatalytic region of tyrosine kinase adaptor protein 1 | Up |
| Fcer1 g | Fc receptor, IgE, high affinity I, gamma polypeptide | Up |
| Retn | Resistin | Up |
| Gnat2 | Guanine nucleotide binding protein, alpha transducing 2 | Up |
| Ufd1l | Ubiquitin fusion degradation 1 like | Up |
| Pnpla2 | Patatin-like phospholipase domain-containing 2 | Up |
| Adcy4 | Adenylate cyclase 4 | Up |
| Nol7 | Nucleolar protein 7 | Up |
| Ccl9 | Chemokine (C–C motif) ligand 9 | Up |
| Ccng1 | Cyclin G1 | Up |
| Gpn2 | GPN-loop GTPase 2 | Up |
| Guk1 | Guanylate kinase 1 | Up |
| Pon3 | Paraoxonase 3 | Up |
| Vps72 | Vacuolar protein sorting 72 (yeast) | Up |
| Bysl | Bystin like | Up |
| Cidec | Cell death-inducing DFFA-like effector c | Up |
| Ell2 | Elongation factor RNA polymerase II 2 | Up |
| Mapk9 | Mitogen-activated protein kinase 9 | Up |
| Prim1 | DNA primase, p49 subunit | Up |
| Irg1 | Immunoresponsive gene 1 | Up |
| Cog5 | Component of oligomeric golgi complex 5 | Up |
| Gk5 | Glycerol kinase 5 (putative) | Up |
| Thumpd1 | THUMP domain-containing 1 | Up |
| Mfge8 | Milk fat globule-EGF factor 8 protein | Up |
| Il2rb | Interleukin-2 receptor, beta chain | Up |
| Dgcr14 | DiGeorge syndrome critical region gene 14 | Up |
| Lingo1 | Leucine-rich repeat and Ig domain-containing 1 | Up |
| S100a3 | S100 calcium binding protein A3 | Up |
| Cdc5l | Cell division cycle 5 like (*S. pombe*) | Up |
| Sepn1 | Selenoprotein N, 1 | Up |
| Rnf215 | Ring finger protein 215 | Up |
| Ywhaq | Tyrosine 3-monooxygenase/tryptophan 5-monooxygenase activation protein, theta polypeptide | Up |
| Rtf1 | Rtf1, Paf1/RNA polymerase II complex component, homolog (*S. cerevisiae*) | Up |
| Itpk1 | Inositol 1,3,4-triphosphate 5/6 kinase | Up |
| Tnk2 | Tyrosine kinase, nonreceptor, 2 | Up |
| Lynx1 | Ly6/neurotoxin 1 | Up |
| Ccl27a | Chemokine (C–C motif) ligand 27A | Up |
| Gkn2 | Gastrokine 2 | Up |
| Psme4 | Proteasome (prosome, macropain) activator subunit 4 | Up |
| Cpsf4l | Cleavage and polyadenylation specific factor 4-like | Up |
| Lefty1 | Left-right determination factor 1 | Up |
| Ambra1 | Autophagy/beclin 1 regulator 1 | Up |
| Btg4 | B cell translocation gene 4 | Up |
| Mapre1 | Microtubule-associated protein, RP/EB family, member 1 | Up |
| Bcar1 | Breast cancer anti-estrogen resistance 1 | Up |
| Exoc4 | Exocyst complex component 4 | Up |
| Nudt14 | Nudix (nucleoside diphosphate-linked moiety X)-type motif 14 | Up |
| Magoh | Mago-nashi homolog, proliferation associated (*Drosophila*) | Up |
| Cr1l | Complement component (3b/4b) receptor 1 like | Up |
| Olfr315 | Olfactory receptor 315 | Up |
| Elane | Elastase, neutrophil expressed | Up |
| Fam158a | Family with sequence similarity 158, member A | Up |
| Acp6 | Acid phosphatase 6, lysophosphatidic | Up |
| Rbm39 | RNA binding motif protein 39 | Up |
| Phf12 | PHD finger protein 12 | Up |
| Retn | Resistin | Up |
| Wdr18 | WD repeat domain 18 | Up |
| Aqr | Aquarius | Up |
| Clk2 | CDC-like kinase 2 | Up |
| Rtf1 | Rtf1, Paf1/RNA polymerase II complex component, homolog (*S. cerevisiae*) | Up |
| Txn1 | Thioredoxin 1 | Up |
| Robo4 | Roundabout homolog 4 (*Drosophila*) | Up |
| Ptpra | Protein tyrosine phosphatase, receptor type, A | Up |
| Pex11a | Peroxisomal biogenesis factor 11 alpha | Up |
| Vegfb | Vascular endothelial growth factor B | Up |
| Pcbp2 | Poly(rC) binding protein 2 | Up |
| Rab11fip5 | RAB11 family interacting protein 5 (class I) | Up |
| Rab8a | RAB8A, member RAS oncogene family | Up |
| Gapdhs | Glyceraldehyde-3-phosphate dehydrogenase, spermatogenic | Up |
| Olfr976 | Olfactory receptor 976 | Up |
| Tnfrsf1b | Tumor necrosis factor receptor superfamily, member 1b | Up |
| Capns2 | Calpain, small subunit 2 | Up |
| Inpp5d | Inositol polyphosphate-5-phosphatase D | Up |
| Tnpo1 | Transportin 1 | Up |
| Rpl35a | Ribosomal protein L35A | Up |
| Nfia | Nuclear factor I/A | Up |
| Ewsr1 | Ewing sarcoma breakpoint region 1 | Up |
| Lamp2 | Lysosomal-associated membrane protein 2 | Up |
| Gmcl1l | Germ cell-less homolog 1 (*Drosophila*) like | Up |
| Krt84 | Keratin 84 | Up |
| Mbtd1 | mbt domain-containing 1 | Up |
| S100a8 | S100 calcium binding protein A8 (calgranulin A) | Up |
| Txnrd2 | Thioredoxin reductase 2 | Up |
| Senp2 | SUMO/sentrin specific peptidase 2 | Up |
| Tpbpa | Trophoblast specific protein alpha | Up |
| Gm13309 | Predicted gene 13309 | Up |
| Csnk2a2 | Casein kinase 2, alpha prime polypeptide | Up |
| Tmem56 | Transmembrane protein 56 | Up |
| Cndp2 | CNDP dipeptidase 2 (metallopeptidase M20 family) | Up |
| Cisd2 | CDGSH iron sulfur domain 2 | Up |
| Rab11b | RAB11B, member RAS oncogene family | Up |
| Sephs1 | Selenophosphate synthetase 1 | Up |
| Cxcl15 | Chemokine (C–X–C motif) ligand 15 | Up |
| Def8 | Differentially expressed in FDCP 8 | Up |
| Pbxip1 | Pre-B cell leukemia transcription factor-interacting protein 1 | Up |
| Pacsin2 | Protein kinase C and casein kinase substrate in neurons 2 | Up |
| Kif1b | Kinesin family member 1B | Up |
| Al316807 | Expressed sequence Al316807 | Up |
| Itk | IL2-inducible T cell kinase | Up |
| Oca2 | Oculocutaneous albinism II | Up |
| Zscan12 | Zinc finger and SCAN domain-containing 12 | Up |
| Adcy6 | Adenylate cyclase 6 | Up |
| Gsn | Gelsolin | Up |
| Dok2 | Docking protein 2 | Up |
| Oxct1 | 3-Oxoacid CoA transferase 1 | Up |
| Apoa1 | Apolipoprotein A-I | Up |
| Ppp1r15a | Protein phosphatase 1, regulatory (inhibitor) subunit 15A | Up |
| Zfp365 | Zinc finger protein 365 | Up |

(*continued*)

**Table 2.** (*Continued*)

(*continued*)

**Table 2. (*Continued*)**

| *Gene Symbol* | *Gene Name* | *Regulation* |
|---|---|---|
| Eci1 | Enoyl-Coenzyme A delta isomerase 1 | Up |
| Gtsf1 | Gametocyte specific factor 1 | Up |
| Pole4 | Polymerase (DNA directed), epsilon 4 (p12 subunit) | Up |
| Trmt1 | TRM1 tRNA methyltransferase 1 homolog (*S. cerevisiae*) | Up |
| Rere | Arginine-glutamic acid dipeptide (RE) repeats | Down |
| Pabpn1 | Poly(A) binding protein, nuclear 1 | Down |
| Nras | Neuroblastoma ras oncogene | Down |
| Dnajb11 | DnaJ (Hsp40) homolog, subfamily B, member 11 | Down |
| Tmcc3 | Transmembrane and coiled-coil domains 3 | Down |
| Atg14 | VATG14 autophagy related 14 homolog (*S. cerevisiae*) | Down |
| Fn1 | Fibronectin 1 | Down |
| Zfp706 | Zinc finger protein 706 | Down |
| Sparc | Secreted acidic cysteine rich glycoprotein | Down |
| Ptbp2 | Polypyrimidine tract binding protein 2 | Down |
| Exoc4 | Exocyst complex component 4 | Down |
| Tmem186 | Transmembrane protein 186 | Down |
| Snx4 | Sorting nexin 4 | Down |
| Ndfip1 | Nedd4 family-interacting protein 1 | Down |
| Rpl10 | Ribosomal protein 10 | Down |
| Ldha | Lactate dehydrogenase A | Down |
| Usp16 | Ubiquitin-specific peptidase 16 | Down |
| Rbmxrt | RNA binding motif protein, X chromosome retrogene | Down |
| Ube2i | Ubiquitin-conjugating enzyme E2I | Down |
| Psmd10 | Proteasome (prosome, macropain) 26S subunit, non-ATPase, 10 | Down |
| Dab2 | Disabled homolog 2 (*Drosophila*) | Down |
| Cdo1 | Cysteine dioxygenase 1, cytosolic | Down |
| Snta1 | Syntrophin, acidic 1 | Down |
| Rpl6 | Ribosomal protein L6 | Down |
| Ing1 | Inhibitor of growth family, member 1 | Down |
| Ldhb | Lactate dehydrogenase B | Down |
| Rps5 | Ribosomal protein S5 | Down |
| Ddx3x | DEAD/H (Asp–Glu–Ala–Asp/His) box polypeptide 3, X-linked | Down |
| Gm7536 | Predicted gene 7536 | Down |
| Mmgt2 | Membrane magnesium transporter 2 | Down |
| Zfp706 | Zinc finger protein 706 | Down |
| Hsd3b7 | Hydroxy-delta-5-steroid dehydrogenase, 3 beta- and steroid delta-isomerase 7 | Down |
| Gm13072 | tRNA methyltransferase 11–2 homolog pseudogene | Down |
| Asah1 | *N*-acylsphingosine amidohydrolase 1 | Down |
| Birc3 | Baculoviral IAP repeat-containing 3 | Down |
| Atp5 g3 | ATP synthase, H+ transporting, mitochondrial F0 complex, subunit C3 (subunit 9) | Down |
| Crabp2 | Cellular retinoic acid binding protein II | Down |
| Clec14a | C-type lectin domain family 14, member a | Down |
| Arhgap4 | Rho GTPase activating protein 4 | Down |
| Ikbkb | Inhibitor of kappa B kinase beta | Down |
| Commd10 | COMM domain containing 10 | Down |
| Tdp1 | Tyrosyl-DNA phosphodiesterase 1 | Down |
| Myh3 | Myosin, heavy polypeptide 3, skeletal muscle, embryonic | Down |
| Aarsd1 | Alanyl-tRNA synthetase domain containing 1 | Down |
| Fndc3b | Fibronectin type III domain containing 3B | Down |
| Kpna3 | Karyopherin (importin) alpha 3 | Down |
| Prl8a2 | Prolactin family 8, subfamily a, member 2 | Down |
| Yap1 | Yes-associated protein 1 | Down |
| Cyp4f39 | Cytochrome P450, family 4, subfamily f, polypeptide 39 | Down |

(*continued*)

**Table 2. (*Continued*)**

| *Gene Symbol* | *Gene Name* | *Regulation* |
|---|---|---|
| Vgll3 | Vestigial like 3 (*Drosophila*) | Down |
| Kpna1 | Karyopherin (importin) alpha 1 | Down |
| Hspa8 | Heat shock protein 8 | Down |
| Usp47 | Ubiquitin specific peptidase 47 | Down |
| B3galnt2 | UDP-GalNAc:betaGlcNAc beta 1,3-galactosaminyltransferase, polypeptide 2 | Down |
| Mmp14 | Matrix metallopeptidase 14 (membrane-inserted) | Down |
| Wnt4 | Wingless-related MMTV integration site 4 | Down |
| Kcnq4 | Potassium voltage-gated channel, subfamily Q, member 4 | Down |
| Rer1 | RER1 retention in endoplasmic reticulum 1 homolog (*S. cerevisiae*) | Down |
| Tspan13 | Tetraspanin 13 | Down |
| Glud1 | Glutamate dehydrogenase 1 | Down |
| Mcmbp | MCM (minichromosome maintenance deficient) binding protein | Down |
| Ranbp1 | RAN binding protein 1 | Down |
| Gm12918 | Predicted gene 12918 | Down |
| P4ha2 | Procollagen-proline, 2-oxoglutarate 4-dioxygenase (proline 4-hydroxylase), alpha II polypeptide | Down |
| Zfyve21 | Zinc finger, FYVE domain containing 21 | Down |
| Homer2 | Homer homolog 2 (*Drosophila*) | Down |
| Fastkd2 | FAST kinase domains 2 | Down |
| Gapdh | Glyceraldehyde-3-phosphate dehydrogenase | Down |
| Ak3 | Adenylate kinase 3 | Down |
| Ppp3r1 | Protein phosphatase 3, regulatory subunit B, alpha isoform (calcineurin B, type I) | Down |
| Rbp7 | Retinol binding protein 7, cellular | Down |
| Mllt3 | Translocated to, 3 | Down |
| Gstk1 | Glutathione S-transferase kappa 1 | Down |
| Mpdu1 | Mannose-P-dolichol utilization defect 1 | Down |
| Ccnb1 | Cyclin B1 | Down |
| Ccbl1 | Cysteine conjugate-beta lyase 1 | Down |
| Son | Son DNA binding protein | Down |
| Ak4 | Adenylate kinase 4 | Down |
| Trim44 | Tripartite motif-containing 44 | Down |
| Lmf1 | Lipase maturation factor 1 | Down |
| Klhl9 | Kelch-like 9 (*Drosophila*) | Down |
| Snap23 | Synaptosomal-associated protein 23 | Down |
| Asb11 | Ankyrin repeat and SOCS box-containing 11 | Down |
| Mrps9 | Mitochondrial ribosomal protein S9 | Down |
| Zrsr2 | Zinc finger (CCCH type), RNA binding motif and serine/arginine rich 2 | Down |
| Tkt | Transketolase | Down |
| Mapk9 | Mitogen-activated protein kinase 9 | Down |
| Kcne2 | Potassium voltage-gated channel, Isk-related subfamily, gene 2 | Down |
| Sirt5 | Sirtuin 5 (silent mating type information regulation 2 homolog) 5 (*S. cerevisiae*) | Down |
| Slc25a11 | Solute carrier family 25 (mitochondrial carrier oxoglutarate carrier), member 11 | Down |
| Fbln1 | Fibulin 1 | Down |
| Gjb6 | Gap junction protein, beta 6 | Down |
| Cnot10 | CCR4-NOT transcription complex, subunit 10 | Down |
| Rbm5 | RNA binding motif protein 5 | Down |
| Car2 | Carbonic anhydrase 2 | Down |
| Lad1 | Ladinin | Down |
| S100a10 | S100 calcium binding protein A10 (calpactin) | Down |
| Parm1 | Prostate androgen-regulated mucin-like protein 1 | Down |
| Dffb | DNA fragmentation factor, beta subunit | Down |
| G3bp2 | GTPase-activating protein (SH3 domain) binding protein 2 | Down |

(*continued*)

**Table 2.** (*Continued*)

| *Gene Symbol* | *Gene Name* | *Regulation* |
|---|---|---|
| Pcmt1 | protein-L-isoaspartate (D-aspartate) *O*-methyltransferase 1 | Down |
| CACNA1S | Calcium channel, voltage-dependent, L type, alpha 1S subunit | Down |
| Grpel2 | GrpE-like 2, mitochondrial | Down |
| Stxbp2 | Syntaxin binding protein 2 | Down |
| Sf3b3 | Splicing factor 3b, subunit 3 | Down |
| Wdr13 | WD repeat domain 13 | Down |
| Tecr | Trans-2,3-enoyl-CoA reductase | Down |
| Ccnd3 | Cyclin D3 | Down |
| Itgb1 | Integrin beta 1 (fibronectin receptor beta) | Down |
| Dab2 | Disabled homolog 2 (*Drosophila*) | Down |
| Ankrd46 | Ankyrin repeat domain 46 | Down |
| Tmem45a | Transmembrane protein 45a | Down |
| Cacng1 | Calcium channel, voltage-dependent, gamma subunit 1 | Down |
| Aldoa | Aldolase A, fructose bisphosphate | Down |
| Ceacam13 | Carcinoembryonic antigen-related cell adhesion molecule 13 | Down |
| Dct | Dopachrome tautomerase | Down |
| Mrps27 | Mitochondrial ribosomal protein S27 | Down |
| Rcbtb2 | Regulator of chromosome condensation (RCC1) and BTB (POZ) domain containing protein 2 | Down |
| Lage3 | L antigen family, member 3 | Down |
| Tbc1d14 | TBC1 domain family, member 14 | Down |
| Bax | BCL2-associated X protein | Down |
| Adrb2 | Adrenergic receptor, beta 2 | Down |
| Rnf6 | Ring finger protein (C3H2C3 type) 6 | Down |
| Hspa5 | Heat shock protein 5 | Down |
| Mt2 | Metallothionein 2 | Down |
| Fam38a | Family with sequence similarity 38, member A | Down |
| Mat2a | Methionine adenosyltransferase II, alpha | Down |
| Ankle2 | Ankyrin repeat and LEM domain containing 2 | Down |
| Prrg4 | Proline rich Gla (G-carboxyglutamic acid) 4 (transmembrane) | Down |
| Tceal7 | Transcription elongation factor A (SII)-like 7 | Down |
| Isca1 | Iron-sulfur cluster assembly 1 homolog (*S. cerevisiae*) | Down |
| Pole2 | Polymerase (DNA directed), epsilon 2 (p59 subunit) | Down |
| Sema4a | Sema domain, immunoglobulin domain (Ig), transmembrane domain (TM), and short cytoplasmic domain, (semaphorin) 4A | Down |
| Ccl6 | Chemokine (C–C motif) ligand 6 | Down |
| Smad1 | MAD homolog 1 (*Drosophila*) | Down |
| Igf2bp1 | Insulin-like growth factor 2 mRNA binding protein 1 | Down |
| Wbp1 | WW domain binding protein 1 | Down |
| Cnot6 | CCR4-NOT transcription complex, subunit 6 | Down |
| Fchsd2 | FCH and double SH3 domains 2 | Down |
| Glcci1 | Glucocorticoid induced transcript 1 | Down |
| Col1a2 | Collagen, type I, alpha 2 | Down |

tRNA, transfer RNA.

of normal dermal architecture. However, in adults, cutaneous wound healing is characterized by physiologic scarring. The goal of this study is to identify candidate pathways important to the scarless wound healing process that might also contribute to decreased scarring and regenerative healing in adult wounds. To achieve this goal, we performed microarray analysis on fetal and adult wounds at three different time points following wounding: 1, 12, and 24 h, to study the temporal activation or suppression of relevant genes to regenerative healing. In addition, to better understand the functionality of observed differential gene regulation, we performed signal pathway analysis. This technique allowed us to identify gene cascades that are regulated during the different phases of wound healing.

**Table 3.** *Differentially expressed genes in E17 fetal versus adult wounds at twenty-four hours postwounding*

| *Gene Symbol* | *Gene Name* | *Regulation* |
|---|---|---|
| Frs2 | Fibroblast growth factor receptor substrate 2 | Up |
| Cdk12 | Cyclin-dependent kinase 12 | Up |
| Serinc3 | Serine incorporator 3 | Up |
| Dct | Dopachrome tautomerase | Up |
| Tars2 | Threonyl-tRNA synthetase 2, mitochondrial (putative) | Up |
| Atg14 | VATG14 autophagy related 14 homolog (*S. cerevisiae*) | Up |
| Rprd1a | Regulation of nuclear pre-mRNA domain containing 1A | Up |
| Pdgfra | Platelet-derived growth factor receptor, alpha polypeptide | Up |
| Mcfd2 | Multiple coagulation factor deficiency 2 | Up |
| Wfdc15b | WAP four-disulfide core domain 15B | Up |
| Ncaph | Non-SMC condensin I complex, subunit H | Up |
| Col1a1 | Collagen, type I, alpha 1 | Down |
| Pdzk1ip1 | PDZK1 interacting protein 1 | Down |
| Zcchc17 | Zinc finger, CCHC domain containing 17 | Down |
| Ctbp2 | C-terminal binding protein 2 | Down |
| Sec31a | Sec31 homolog A (*S. cerevisiae*) | Down |
| Rpl22 | Ribosomal protein L22 | Down |
| Slc46a2 | Solute carrier family 46, member 2 | Down |
| Krt8 | Keratin 8 | Down |
| Igf2bp2 | Insulin-like growth factor 2 mRNA binding protein 2 | Down |
| Dhdds | Dehydrodolichyl diphosphate synthase | Down |
| Abhd14b | Abhydrolase domain containing 14b | Down |
| Krt18 | Keratin 18 | Down |
| Arid4a | AT rich interactive domain 4A (RBP1-like) | Down |
| Necap2 | NECAP endocytosis associated 2 | Down |
| Txndc17 | Thioredoxin domain containing 17 | Down |
| Krt16 | Keratin 16 | Down |

E, embryonic day.

## Updated discoveries in differential gene expression

Using microarray analyses similar to those previously described by Colwell *et al.*, we found 191, 253, and 27 genes that were differentially expressed between E17 fetal and adult wounds at 1, 12, and 24 h postinjury, respectively. E17 was the earliest gestational age where scarless healing occurs,[6,12] and that allowed reproducible and reliable survival after surgery. The results represent an overall increase from the 175, 134, and 19 differentially expressed genes, at each respective time point, which were identified in the previous study. With the updated gene database utilized in this new study, we were able to detect not only a more accurate but also expanded set of genes that may

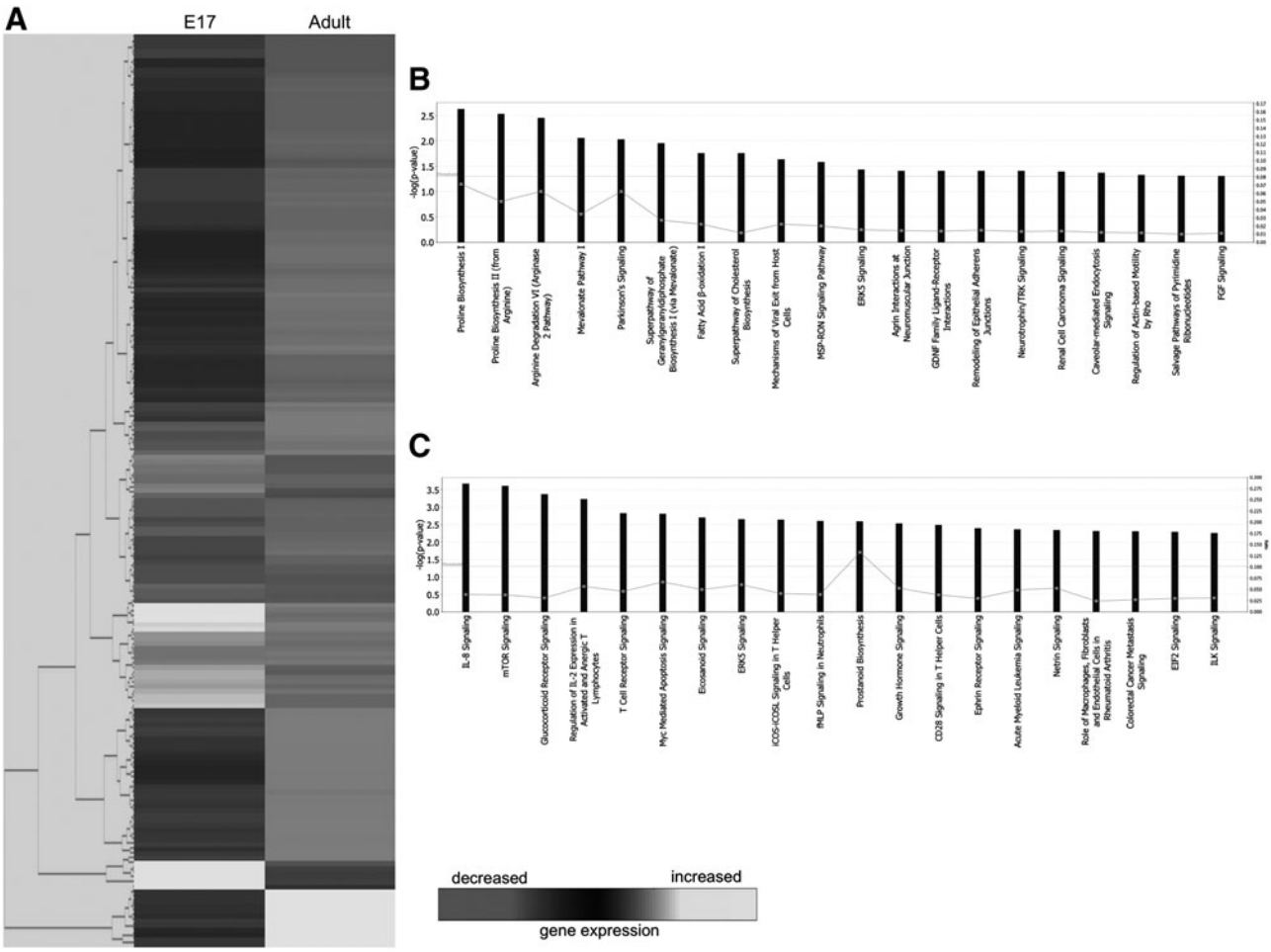


**Figure 1.** Microarray analysis of E17 fetal and adult wounds at 1 h postwounding. **(A)** Hierarchical clustering of differentially regulated genes from E17 fetal and adult wounds at 1 h postwounding. Individual genes are clustering according to the dendrogram on the *left*, and expression levels are represented in the heatmap on the *right*. *White/lighter gray* and *darker gray* indicate upregulation and downregulation, respectively. **(B)** Canonical pathways significantly enriched for among genes whose expression was significantly upregulated in E17 samples compared to adult. **(C)** Canonical pathways significantly enriched for among genes whose expression was significantly downregulated in E17 samples compared to adult. E, embryonic day.

serve as potential candidates for further study in scarless regeneration. Furthermore, improved pathway analysis abilities provided an objective, unified picture of associated functional pathways rather than solely individual genes, thereby further elucidating possible mechanisms in fetal wound healing. Interestingly, our results reveal some pathways that corroborate earlier hypotheses by Colwell *et al.*, such as the upregulation of protein ubiquitination in fetal wounds at 12 h, while providing additional context for understanding specific prior findings, such as the earlier discovery of greater expression of angiomotin and our new association of the intrinsic prothrombin activation pathway in fetal wound healing 24 h postinjury.

The phenotype of fetal scarless healing is skin regeneration that cannot be differentiated from unwounded skin. Collagen deposition is unchanged and dermal appendages are present after fetal scarless repair. Although our analyses did not solely focus on the phenotypic sequelae, we identified myriad genes and pathways that may play a role in regeneration. Below, we discuss in greater detail some of the most relevant pathways found to be differentially activated in E17 fetal versus adult wounds at various time points following injury. Although the potential roles of these pathways are discussed individually, they may interact together. Such potential interactions are yet unknown and not discussed in this article.

### Proline biosynthesis I

The proline biosynthesis I pathway in humans cumulates with the synthesis of L-proline. Proline, a major component of collagen and hydroxyproline, found in only a few other proteins in vertebrates, is

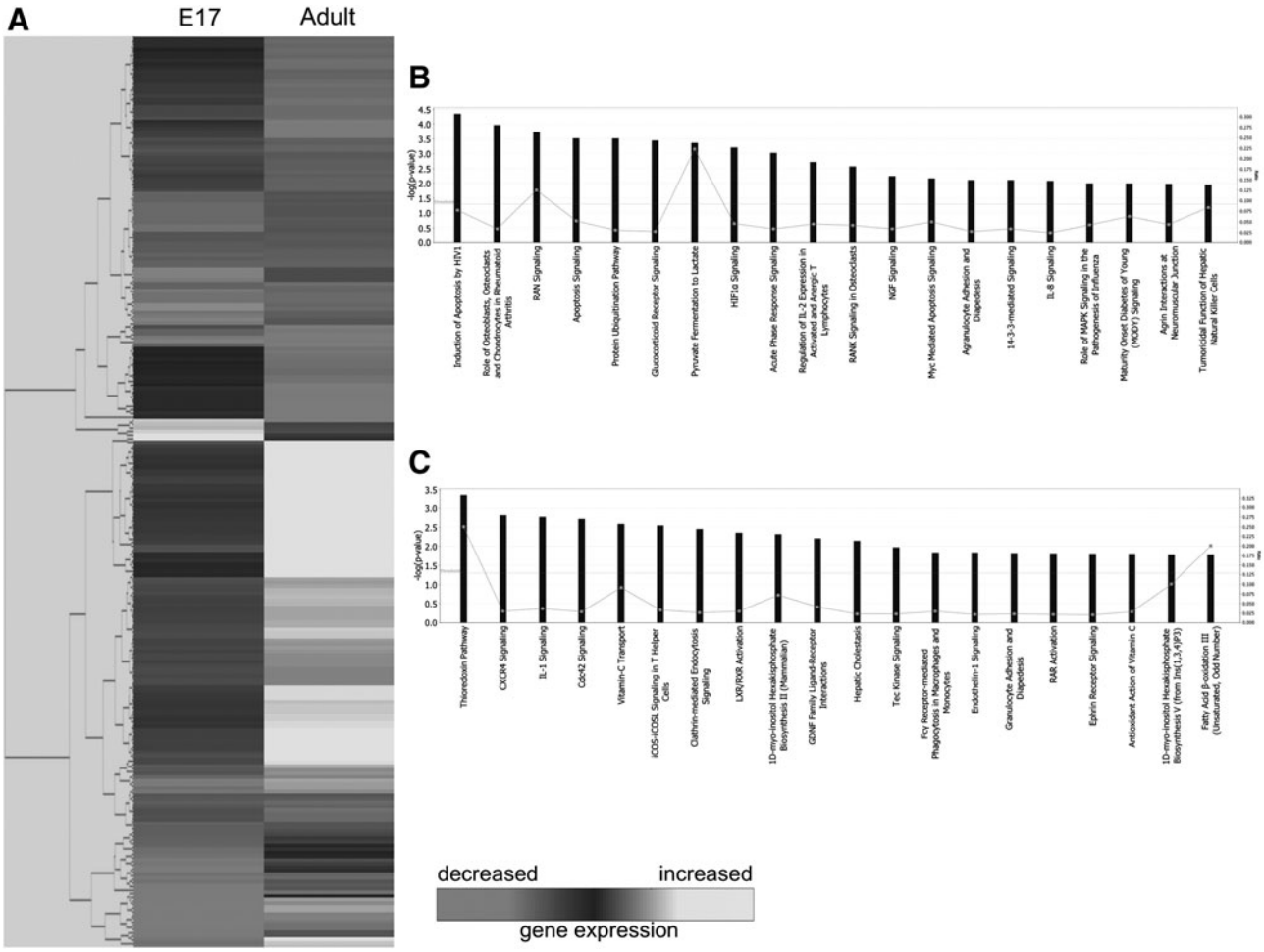


**Figure 2.** Microarray analysis of E17 fetal and adult wounds at 12 h postwounding. **(A)** Hierarchical clustering of differentially regulated genes from E17 fetal and adult wounds at 12 h postwounding. Individual genes are clustering according to the dendrogram on the *left,* and expression levels are represented in the heatmap on the *right. White/lighter gray* and *darker gray* indicate upregulation and downregulation, respectively. **(B)** Canonical pathways significantly enriched for among genes whose expression was significantly upregulated in E17 samples compared to adult. **(C)** Canonical pathways significantly enriched for among genes whose expression was significantly downregulated in E17 samples compared to adult.

essential to the stabilization of the collagen triple helix.[14] As such, the proline biosynthetic pathway can correspondingly contribute to the modulation of wound healing and scar formation. An hour after wounding, our results demonstrated markedly increased activation of the proline biosynthesis pathway in E17 wounds compared to adult wounds. While traditionally excess collagen has been associated with a number of fibrotic disorders, such as lung cirrhosis, excessive scar formation, and cirrhosis of the liver,[15] our results suggest that early upregulation of synthesis of a core component of collagen may actually contribute to scarless regeneration. This may be due to the effect of early upregulation of proline synthesis on the type of collagen deposited or the metabolism of collagen, especially as poly(L-proline) has been found to be an effective competitive inhibitor of vertebrate type I collagen prolyl 4-hydroxylase.[16] However, the exact mechanism underlying this observation remains to be delineated and more studies are required to elucidate means by which early upregulation of proline synthesis contributes to scarless repair.

### IL-8 signaling

In adult wounds, IL-8 has been shown to be primarily responsible for chemotaxis of neutrophils, which contributes to the inflammatory process.[17] While IL-8 is known to stimulate inflammation in adult wound healing, its role in fetal wound healing remains unclear. Our results demonstrate downregulation of IL-8 signaling pathways in fetal wounds 1 h postinjury in comparison to adult wounds. This diminished IL-8 pathway activation corresponds to a diminished inflammatory

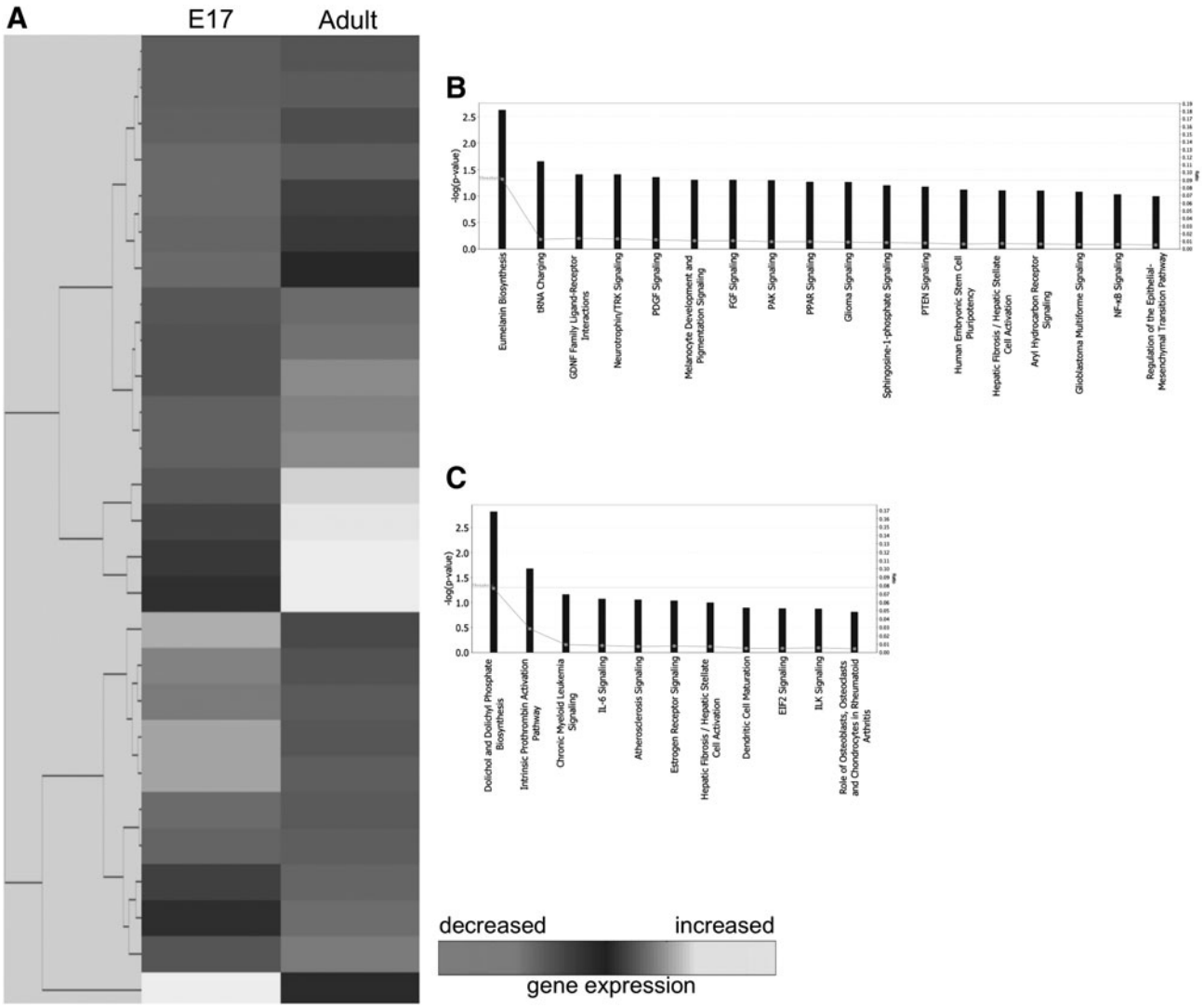


**Figure 3.** Microarray analysis of E17 fetal and adult wounds at 24 h postwounding. **(A)** Hierarchical clustering of differentially regulated genes from E17 fetal and adult wounds at 24 h postwounding. Individual genes are clustering according to the dendrogram on the *left,* and expression levels are represented in the heatmap on the *right. White/lighter gray* and *darker gray* indicate upregulation and downregulation, respectively. **(B)** Canonical pathways significantly enriched for among genes whose expression was significantly downregulated in E17 samples compared to adult. **(C)** Canonical pathways significantly enriched for among genes whose expression was significantly upregulated in E17 samples compared to adult.

response commonly found in fetal wounds as well as the lack of polymorphic leukocyte infiltrate seen in scarless wound healing.[18] Less inflammatory cell recruitment and diminished cytokine release have been suggested to cause decreased paracrine stimulation of extracellular matrix production, as well as increased fibroblast and epithelial cell migration and proliferation.[17] Thus, this lack of inflammatory cascade amplification may be crucial to the formation of an environment conducive to scarless wound healing. Last, excessive IL-8 has been found in disease states characterized by excessive fibroplasia, such as pulmonary fibrosis[19] and psoriasis,[20] further underscoring its contribution to profibrotic processes.

### Apoptosis signaling

Apoptosis is critical to the normal progression of wound healing. Especially, as the wound matures, apoptosis plays an important role in the regulation of collagen synthesis and degradation through its regulation of fibroblast and endothelial cell death. Our results indicate that E17 fetal wounds demonstrated upregulation of apoptosis signaling pathways 12 h following wounding in comparison to adult counterparts. This finding is supported by published studies demonstrating a role for increased induction of apoptosis in fibroblast populations as a possible mechanism for promotion of scarless wound healing.[21] Furthermore, recent studies have suggested that decreased rates of

apoptosis in mice may lead to the formation of hypertrophic scars and keloids.[22] Taken together, these data suggest that initiation of apoptosis following injury may contribute to scarless wound healing through the programmed removal of damaged and unwanted cells at the site of injury.

### CXCR4 pathway

CXCR4 encodes the receptor for stromal cell-derived factor-1 (SDF-1), which acts as a potent chemoattractant for lymphocytes and monocytes[23] and is further responsible for the trafficking of circulating stem and progenitor cells to areas of tissue damage during cutaneous wound repair.[24,25] SDF-1 is often induced by proinflammatory factors, such as tumor necrosis factor-$\alpha$ (TNF-$\alpha$) and IL-1,[26] and has also been found in elevated levels in fibrotic disorders. Our results demonstrate upregulation of CXCR4 pathway in adult wounds 12 h following injury in comparison to fetal wounds. This finding is in concordance with recent experimental data suggesting that the activation of SDF-1 signaling by proinflammatory factors recruits cells expressing CXCR4 such as fibrocytes, which contribute to the formation of hypertrophic scars.[26] The regulation of SDF-1 and CXCR4 thus provides an important ligand-receptor target for reducing scarring through inhibition of fibrocyte trafficking.

### Neurotrophin/TRK signaling

Neurotrophin is synthesized and released by many skin cells, including keratinocytes, melanocytes, and fibroblasts.[27] In skin, neurotrophins help regulate innervation and act as prosurvival and growth factors. As such, they are believed to play an important role in regulating skin homeostasis in both physiologic and pathologic states. Data from our pathway analysis indicate that neurotrophin and its receptor TRK signaling are upregulated in adult wounds 24 h postinjury in comparison to E17 fetal wounds, and as such may play an important role in scar formation. This finding is supported by studies showing that neurotrophin acts to recruit fibroblasts. In addition, injury and inflammation both act to enhance neurotrophin production, mainly by keratinocytes at the site of injury, supporting the role of neurotrophin signaling during wound repair.[28] Altered levels of neurotrophin signaling may thus be expected to contribute to adult scar formation, although no studies to date have looked at this relationship.

### Intrinsic prothrombin activation pathway

Thrombin, which is produced from prothrombin, enhances the production of cytokines such as IL-1, 6, and 8, and TNF-$\alpha$ to upregulate the production of growth factors that in turn induce cellular proliferation at the site of injury.[29] This suggests that prothrombin, thrombin, and their receptors may be responsible for modulating the various phases of scar formation. Our microarray results indicate that the intrinsic prothrombin activation pathway is upregulated in fetal wounds 24 h following wounding in comparison to the adult. Increased levels of thrombin and prothrombin have been found in old scars, suggesting that these proteins play an extended role in wound healing beyond the more immediate coagulation following injury. The unexpected result that this pathway is more active during scarless repair suggests an unknown function during extracellular matrix formation and remodeling. Interestingly, studies have found that the administration of thrombin peptides to incisional wounds in rats accelerates normal wound healing and enhances neovascularization.[30] However, more studies are required to delineate the exact mechanisms by which differential activation of this pathway contributes to scarring versus regeneration.

## INNOVATION

Using functional pathway analysis, we demonstrated differential pathway regulation in E17 fetal wounds that undergo scarless regeneration following injury. Due to the large amount of data generated by pathway analysis, we have limited our discussion to pathways known to be particularly relevant to wound healing. We believe that identifying these pathways most likely to be proregenerative or profibrotic provides a valuable foundation for further experimental study investigating mechanisms underlying the regenerative ability of early embryonic skin, with possible applications to other organ systems.

## ACKNOWLEDGMENTS AND FUNDING SOURCES

This work was supported, in part, by a grant from NIH grant R01 GM087609 (to H.P.L.), a Gift from Ingrid Lai and Bill Shu in honor of Anthony Shu (to H.P.L.), the Hagey Laboratory for Pediatric Regenerative Medicine and Children's Surgical Research Program (to M.T.L. and H.P.L.), and NIH grant R01 GM116892 (to M.T.L. and H.P.L.). Additional funding was provided by the American Society of Maxillofacial Surgeons (ASMS)/Maxillofacial Surgeons Foundation (MSF) Research Grant Award (to M.S.H., M.T.L., and H.P.L.), the

Sarnoff Cardiovascular Research Foundation (to W.X.H.), the California Institute for Regenerative Medicine (CIRM) Clinical Fellow training grant TG2-01159 (to M.S.H.), and the Stanford University School of Medicine Transplant and Tissue Engineering Fellowship Award (to M.S.H.).

## AUTHOR DISCLOSURE AND GHOSTWRITING

No competing financial interests exist. The content of this article was expressly written by the authors listed. No ghostwriters were used to write this article.

## KEY FINDINGS

- We identified 471 differentially expressed genes between fetal and adult wounds.
- Enrichment analysis revealed 109 signaling pathways related to fetal scarless repair.
- Twenty signaling pathways were upregulated and downregulated at 1 and 12 h after injury.
- Twenty-four hours after injury, 18 signaling pathways were upregulated in adult wounds and 11 pathways were downregulated compared to fetal wounds.

## ABOUT THE AUTHORS

**Michael S. Hu, MD, MPH, MS,** is a postdoctoral fellow at Stanford pursuing a career in plastic surgery. **Wan Xing Hong, MD, MS,** is a general surgery resident. **Michael Januszyk**, **MD, PhD, Anna Luan, MD, Zeshaan N. Maan, MD, Shawn Moshrefi, MD, and Ruth Tevlin, MB, BCh, BAO, MRCSI,** are plastic surgery residents. **Graham G. Walmsley, MD, PhD,** is a stem cell scientist working in venture capital. **Derrick C. Wan, MD,** is an associate professor of plastic surgery. **Geoffrey C. Gurtner, MD,** and **Michael T. Longaker, MD, MBA** are professors of surgery. **H. Peter Lorenz, MD** is a Professor and Chief of Plastic Surgery at the Lucile Packard Children's Hospital at Stanford. His clinical interests are in craniofacial surgery, pediatric plastic surgery, and reconstructive and cosmetic surgery. His laboratory group is studying mechanisms underlying scarless skin healing and the function of progenitor cells during wound repair/regeneration.

## REFERENCES

1. Rowlatt U. Intrauterine wound healing in a 20 week human fetus. Virchows Arch A Pathol Anat Histol 1979;381:353–361.
2. Lorenz HP, Longaker MT, Perkocha LA, Jennings RW, Harrison MR, Adzick NS. Scarless wound repair: a human fetal skin model. Development 1992;114:253–259.
3. Lorenz HP, Whitby DJ, Longaker MT, Adzick NS. Fetal wound healing. The ontogeny of scar formation in the non-human primate. Ann Surg 1993; 217:391–396.
4. Beanes SR, Hu FY, Soo C, Dang CM, Urata M, Ting K, et al. Confocal microscopic analysis of scarless repair in the fetal rat: defining the transition. Plast Reconstr Surg 2002;109:160–170.
5. Buchanan EP, Longaker MT, Lorenz HP. Fetal skin wound healing. Adv Clin Chem 2009;48:137–161.
6. Colwell AS, Longaker MT, Peter Lorenz H. Identification of differentially regulated genes in fetal wounds during regenerative repair. Wound Repair Regen 2008;16:450–459.
7. Singer AJ, Clark RA. Cutaneous wound healing. N Engl J Med 1999;341:738–746.
8. Lo DD, Zimmermann AS, Nauta A, Longaker MT, Lorenz HP. Scarless fetal skin wound healing update. Birth Defects Res C Embryo Today 2012; 96:237–247.
9. Gurtner GC, Werner S, Barrandon Y, Longaker MT. Wound repair and regeneration. Nature 2008;453: 314–321.
10. Shih B, Garside E, McGrouther DA, Bayat A. Molecular dissection of abnormal wound healing processes resulting in keloid disease. Wound Repair Regen 2010;18:139–153.
11. Walmsley GG, Hu MS, Hong WX, Maan ZN, Lorenz HP, Longaker MT. A mouse fetal skin model of scarless wound repair. J Vis Exp 2015:52297.
12. Colwell AS, Krummel TM, Longaker MT, Lorenz HP. An in vivo mouse excisional wound model of scarless healing. Plast Reconstr Surg 2006;117: 2292–2296.
13. Hu MS, Januszyk M, Hong WX, Walmsley GG, Zielins ER, Atashroo DA, et al. Gene expression in fetal murine keratinocytes and fibroblasts. J Surg Res 2014;190:344–357.
14. Prockop DJ, Kivirikko KI, Tuderman L, Guzman NA. The biosynthesis of collagen and its disorders (first of two parts). N Engl J Med 1979;301:13–23.
15. Zimny M, Klosterhalfen B, Conze J, Hamacher K, Fehler S, Schumpelick V, et al. Uptake of cis-4-[18 F]fluoro-L-proline in scar formation: a marker of collagen synthesis? Nucl Med Commun 2002;23: 695–698.
16. Myllyharju J, Kivirikko KI. Identification of a novel proline-rich peptide-binding domain in prolyl 4-hydroxylase. EMBO J 1999;18:306–312.
17. Liechty KW, Crombleholme TM, Cass DL, Martin B, Adzick NS. Diminished interleukin-8 (IL-8) production in the fetal wound healing response. J Surg Res 1998;77:80–84.
18. Hu MS, Maan ZN, Wu JC, Rennert RC, Hong WX, Lai TS, et al. Tissue engineering and regenerative repair in wound healing. Ann Biomed Eng 2014; 42:1494–1507.
19. Vaillant P, Menard O, Vignaud JM, Martinet N, Martinet Y. The role of cytokines in human lung fibrosis. Monaldi Arch Chest Dis 1996;51:145–152.
20. Konstantinova NV, Duong DM, Remenyik E, Hazarika P, Chuang A, Duvic M. Interleukin-8 is induced in skin equivalents and is highest in those derived from psoriatic fibroblasts. J Invest Dermatol 1996;107:615–621.
21. Abe M, Yokoyama Y, Ishikawa O. A possible mechanism of basic fibroblast growth factor-promoted scarless wound healing: the induction

of myofibroblast apoptosis. Eur J Dermatol 2012; 22:46–53.

22. Aarabi S, Bhatt KA, Shi Y, Paterno J, Chang EI, Loh SA, et al. Mechanical load initiates hypertrophic scar formation through decreased cellular apoptosis. FASEB J 2007;21:3250–3261.
23. Bleul CC, Fuhlbrigge RC, Casasnovas JM, Aiuti A, Springer TA. A highly efficacious lymphocyte chemoattractant, stromal cell-derived factor 1 (SDF-1). J Exp Med 1996;184:1101–1109.
24. Zong ZW, Cheng TM, Su YP, Ran XZ, Shen Y, Li N, et al. Recruitment of transplanted dermal multipotent stem cells to sites of injury in rats with combined radiation and wound injury by interaction of SDF-1 and CXCR4. Radiat Res 2008;170: 444–450.
25. Ceradini DJ, Kulkarni AR, Callaghan MJ, Tepper OM, Bastidas N, Kleinman ME, et al. Progenitor cell trafficking is regulated by hypoxic gradients through HIF-1 induction of SDF-1. Nat Med 2004; 10:858–864.
26. Ding J, Hori K, Zhang R, Marcoux Y, Honardoust D, Shankowsky HA, et al. Stromal cell-derived factor 1 (SDF-1) and its receptor CXCR4 in the formation of postburn hypertrophic scar (HTS). Wound Repair Regen 2011;19:568–578.
27. Palazzo E, Marconi A, Truzzi F, Dallaglio K, Petrachi T, Humbert P, et al. Role of neurotrophins on dermal fibroblast survival and differentiation. J Cell Physiol 2012;227:1017–1025.
28. Peters EM, Raap U, Welker P, Tanaka A, Matsuda H, Pavlovic-Masnicosa S, et al. Neurotrophins act as neuroendocrine regulators of skin homeostasis in health and disease. Horm Metab Res 2007;39: 110–124.
29. Artuc M, Hermes B, Algermissen B, Henz BM. Expression of prothrombin, thrombin and its receptors in human scars. Exp Dermatol 2006;15:523–529.
30. Carney DH, Mann R, Redin WR, Pernia SD, Berry D, Heggers JP, et al. Enhancement of incisional wound healing and neovascularization in normal rats by thrombin and synthetic thrombin receptor-activating peptides. J Clin Invest 1992;89:1469–1477.

**Abbreviations and Acronyms**

cDNA = complementary DNA
CXCR = CXC chemokine receptor
E = embryonic day
IL = interleukin
NIH = National Institutes of Health
PBS = phosphate-buffered saline
SAM = significance analysis of microarrays
SDF-1 = stromal cell-derived factor-1
TNF-$\alpha$ = tumor necrosis factor-$\alpha$
TRK = tropomyosin receptor kinase
tRNA = transfer RNA